

# Naval Research Laboratory

Washington, DC 20375-5000



NRL/MR/4404-92-6961

AD-A248 634



## Computations of Detonation Structure: The Influence of Model Input Parameters

MICHEL H. LEFEBVRE

*Department of Chemistry  
Polytechnic Institute  
Royal Military Academy  
Brussels, Belgium*

ELAINE S. ORAN AND K. KAILASANATH

*Laboratory for Computational Physics and Fluid Dynamics*

April 10, 1992



92-09908



Approved for public release; distribution unlimited.

92 4 17 071

REPORT DOCUMENTATION PAGE			Form Approved OMB No. 0704-0188	
Public reporting burden for this collection of information is estimated to average 1 hour per response, including the time for reviewing instructions, searching existing data sources, gathering and maintaining the data needed, and completing and reviewing the collection of information. Send comments regarding this burden estimate or any other aspect of this collection of information, including suggestions for reducing this burden, to Washington Headquarters Services, Directorate for Information Operations and Reports, 1215 Jefferson Davis Highway, Suite 1204, Arlington, VA 22202-4302, and to the Office of Management and Budget, Paperwork Reduction Project (0704-0188), Washington, DC 20503				
1. AGENCY USE ONLY (Leave blank)	2. REPORT DATE April 10, 1992	3. REPORT TYPE AND DATES COVERED Interim		
4. TITLE AND SUBTITLE Computations of Detonation Structure: The Influence of Model Input Parameters		5. FUNDING NUMBERS		
6. AUTHOR(S) Michel H. Lefebvre, Elaine S. Oran, and K. Kailasanath				
7. PERFORMING ORGANIZATION NAME(S) AND ADDRESS(ES) Naval Research Laboratory Washington, DC 20375-5000		8. PERFORMING ORGANIZATION REPORT NUMBER NRL/MR/4404-92-6961		
9. SPONSORING / MONITORING AGENCY NAME(S) AND ADDRESS(ES) Office of the Chief of Naval Research 800 North Quincy Street, BCT # 1 Arlington, VA 22217-5000		10. SPONSORING / MONITORING AGENCY REPORT NUMBER		
11. SUPPLEMENTARY NOTES				
12a. DISTRIBUTION / AVAILABILITY STATEMENT Approved for public release; distribution unlimited.		12b. DISTRIBUTION CODE		
13. ABSTRACT (Maximum 200 words)  We describe analyses and numerical computations that examine the validity of certain common simplifications in the chemical and thermophysical model on the calculation of detonation properties. In particular, we examine the effects of (1) approximations of the temperature dependence of the specific heat $C_p$ , and the ratio of specific heats $\gamma = C_p/C_v$ in a detailed numerical simulation of detonation in a mixture of hydrogen and oxygen mixture, (2) varying the heat release, and (3) varying the chemical induction time, and compare all of those approximations to a computation that uses a detailed model of the chemical kinetics and correct thermophysics. Finally, we describe computations of detonations in mixtures of hydrogen and oxygen diluted with argon and carbon tetrafluoride and show how the numerical model correctly predicts the trends in the detonation velocity as the percentage of carbon tetrafluoride is increased.				
14. SUBJECT TERMS Detonation structure                      Detonation Modeling Detonation simulations		15. NUMBER OF PAGES 22		
		16. PRICE CODE		
17. SECURITY CLASSIFICATION OF REPORT UNCLASSIFIED	18. SECURITY CLASSIFICATION OF THIS PAGE UNCLASSIFIED	19. SECURITY CLASSIFICATION OF ABSTRACT UNCLASSIFIED	20. LIMITATION OF ABSTRACT UL	

## CONTENTS

1.	Introduction .....	1
2.	Reference State .....	2
3.	Calculation of Internal Energy, Pressure and Temperature .....	3
	3.1 Full Integration .....	3
	3.2 Constant Heat Capacity Approximation .....	3
	3.3 Comments .....	6
4.	A Detonation in a H <sub>2</sub> -O <sub>2</sub> -Ar Mixture .....	6
	4.1 Numerical Model .....	6
	4.2 Cases Studied .....	7
	4.3 Results and Comments .....	9
5.	Detonations in Mixtures Containing Fluorocarbons .....	10
	5.1 Preliminary Observations .....	10
	5.2 Time-Dependent One-Dimensional Calculations .....	11
	5.3 Comments .....	12
6.	Conclusion .....	13
	Acknowledgments .....	13
	References .....	14

Accession For	
NTIS GSA&I	<input checked="" type="checkbox"/>
DTIC TAB	<input type="checkbox"/>
Unannounced	<input type="checkbox"/>
Justification	
By	
Distribution/	
Availability Codes	
Dist	Avail and/or Special
A-1	

# Computations of Detonation Structure: The Influence of Model Input Parameters

## 1. Introduction

Typical reactive-flow problems solve some form of the equations of conservation of mass, momentum, and energy. The solution of these equations provides the knowledge of the three associated fundamental quantities, that is, density  $\rho$  (kg/m<sup>3</sup>), momentum  $\rho v$  (kg/m<sup>2</sup>s), and density of total energy  $E$  (J/m<sup>3</sup>). The total energy considered is usually defined as the sum of the internal energy and the kinetic energy,

$$E = \rho U + \frac{\rho v^2}{2}, \quad (1)$$

where  $U$  (J/kg) is the internal energy of the system. The internal energy is related to temperature and pressure through the caloric equation of state,

$$U = U(T, P), \quad (2)$$

and temperature (K) and pressure (Pa) are related by the thermal equation of state

$$P = P(T, \rho). \quad (3)$$

In this formulation, variables such as internal energy, temperature, velocity, and pressure are derived quantities. At each stage of the calculation, the internal energy can be calculated using equation (1), and knowing  $U$  and the two equations of state enables us to calculate the pressure and temperature. The pressure is required for the calculation of the source terms in the conservation equations. For example, the temperature is required when chemical and thermal processes are involved.

The calculation of the energy of a system is based on the definition of a 'state' at which the energy is assumed to have a given value, that is, a 'reference state.' Thus we first define this concept as accurately as possible and then discuss the caloric equation of state in its simplest form, that is,

$$U = U(T) = U_f + \int C_v(T) dT,$$

where  $U_f$  is the internal energy of formation and the integral represents the sensible internal energy. This form leads to the use of the ratio of heat capacities,  $\gamma = C_p/C_v$  and automatically limits the use of the material in this report to mixtures of ideal gases. In this paper, we do not consider

other more complex equations, such as  $U = U(\rho, T)$  or  $U(P, T)$ . Then, the relation between the temperature and the pressure is

$$P(T, \rho) = \rho NRT ,$$

where  $N$  is the total number of mol (mol/kg).

In many computations, we use simplified models of the chemistry for which we do not track all of the chemical species that might be involved. For such computations, we need simplified models of  $C_v$ . The question is then how to get the best  $C_v$  model or one that is consistent with the reduced chemical model. The purpose of this report is to describe and to discuss the relations between the internal energy of gaseous mixtures and the temperature and pressure. that is, equation (2). We first focus on theoretical ways to compute the expression  $\int C_v(T) dT$  and then on the temperature dependences of the heat capacity,  $C_v$ , and the ratio of heat capacities,  $\gamma$ . Then the influence of the approximation to  $C_v$  on the derived quantities  $P$  and  $T$  is estimated. In the second part of this work, the influence of the temperature and species dependence of the quantity  $\gamma$  will be studied for the particular case of a one-dimensional simulation of a detonation wave. Finally, we discuss two other chemistry-dependent parameters, namely the heat-release function and the chemical induction time.

## 2. Reference State

Energy (enthalpy) changes are relative quantities, thus we must relate each compound to a reference state which is done by referring each energy (enthalpy) to the chemical elements in their standard reference state. By definition, we assume that a gaseous mixture is in the reference state when:

1. All constituents are in the standard state, that is,  $H_2$  for hydrogen,  $O_2$  for oxygen,  $N_2$  for nitrogen, solid carbon graphite for carbon, etc.
2. A reference temperature,  $T_o$ , is chosen.
3. The pressure is equal to 1 bar (100,000 Pa).

In this reference state, the internal energy (enthalpy) of the mixture is assumed to be equal to zero. We may thus speak about the 'internal energy (enthalpy) of a mixture' instead of the 'change in internal energy (enthalpy) of the mixture.'

### 3. Calculation of the Internal Energy, Temperature, and Pressure

The internal energy of a mixture of ideal gases is given by

$$U(T) = \sum_i n_i u_{fi}^o + \int_{T_o}^T \sum_i n_i c_{vi}(T) dT ,$$

where  $c_{vi}(T)$  is the heat capacity of the species  $i$  at constant volume (J/K mol),  $n_i$  is the number of moles of species  $i$  (mol/kg), and  $u_{fi}^o$  is the molar internal energy of formation of species  $i$  at temperature  $T_o$  (J/mol). If we consider the energy of formation of the whole mixture,  $U_f^o$ , and its global heat capacity,  $C_v$ ,

$$U_f^o = \sum_i n_i u_{fi}^o \quad \text{and} \quad C_v(T) = \sum_i n_i c_{vi}(T) ,$$

we may write

$$U(T) = U_f^o + \int_{T_o}^T C_v(T) dT . \quad (4)$$

It is important to notice that  $U_f^o$  is the energy of formation of the mixture at the chosen reference temperature  $T_o$ . The integral in equation (4) represents the sensible internal energy of the system and can be calculated by full integration or by assuming a temperature-independent value of the heat capacity  $C_v$ . The question is how can we deduce the temperature from a known internal energy  $U(T)$ , using equation (4).

#### 3.1 Full Integration

The unknown temperature is the upper boundary of the integral in equation (4). Usually  $C_v(T)$  is known in the form of a polynomial, so that the integral can be evaluated analytically and  $T$  can be calculated iteratively. In this case, the temperature and species dependence of the internal energy is fully taken into account. The disadvantage of this approach is the time it may take to iterate to the correct solution and the fact that, in this case, the densities of all the species must be tracked. This means solving many complex chemical equations and increases the number of conservation equations.

#### 3.2 Constant Heat Capacity Approximation

In order to save computer time, it is often convenient to use simplified chemical models and a temperature-independent heat capacity  $C_v$ . If we know an average value of the heat capacity of the mixture  $C_v^*$ , we may write

$$U(T) = C_v^* (T - T_o) + U_f^o , \quad (5)$$

or using the average ratio of heat capacities,  $\gamma^* = C_p^*/C_v^*$ ,

$$U(T) = U_f^o - \frac{RT_o}{M(\gamma^* - 1)} + \frac{RT}{M(\gamma^* - 1)} .$$

where  $M$  is the mean molar mass of the gas (g/mol). The total energy density is thus

$$E = \rho U_f^o + \left(1 - \frac{T_o}{T}\right) \frac{P}{\gamma^* - 1} + \frac{\rho v^2}{2} . \quad (6)$$

If the reference temperature is equal to 0K, equation (6) can be simplified, that is,

$$E = \rho U_f^o + \frac{P}{\gamma^* - 1} + \frac{\rho v^2}{2} . \quad (7)$$

In this case ( $T_o = 0$  K), we may use either the internal energy of formation  $U_f^o$  or the enthalpy of formation  $H_f^o$ , since the enthalpy and internal energy of formation are equal at 0 K . Equation (7) is particularly simple and useful. The pressure can be directly calculated from equation (7), and the temperature from the thermal equation of state. The theoretical average value of the heat capacity  $C_v^*$  and its derived variable  $\gamma^*$  are given by

$$C_v^* = \frac{\int_0^T C_v(T) dT}{T} , \quad \text{and} \quad \gamma^* = \frac{(R + C_v^*)}{C_v^*} . \quad (8)$$

If this value of  $\gamma^*$  is used, the pressure computed from equation (7) must be done using the full temperature and species dependence of  $U(T)$ . As  $U(T, n_i)$  is usually not known exactly unless the full chemical and thermodynamic computations are carried out, we still need to have an estimate of  $C_v^*$  or  $\gamma^*$  for simplified chemical models.

We denote the estimated mean values of  $C_v^*$  and  $\gamma^*$  by  $C_v^+$  and  $\gamma^+$ . Then the value of  $\gamma^+$  can be estimated theoretically

- a. As  $\gamma^+ = 1.66$  for a monatomic gas and  $\gamma^+ = 1.40$  for a diatomic gas,
- b. By calculating  $\gamma^+$  at room temperature (298 K) and assuming that  $\gamma^+$  is constant, so that

$$\gamma^+ = \frac{\sum_i n_i C_{v_i,298} + R \sum_i n_i}{\sum_i n_i C_{v_i,298}} = \gamma_{298} . \quad (9)$$

- c. By assuming

$$C_v^+ = \frac{C_{vT} + C_{vT_{298}}}{2} , \quad \text{and} \quad \gamma^+ = \frac{C_v^+ + R/M}{C_v^+} , \quad (10)$$

$$\frac{1}{(\gamma^+ - 1)} = \frac{(\gamma_T - 1)^{-1} + (\gamma_{T_{298}} - 1)^{-1}}{2} , \quad (11)$$

if a reasonable value,  $C_{vT}$  or  $\gamma_T$ , of  $C_v$  or  $\gamma$  at the unknown temperature  $T$  can be estimated.

For the species O<sub>2</sub> and H<sub>2</sub>O, Figures 1 and 2 show four quantities computed using the different approximations of C<sub>v</sub>,

- A. the value of C<sub>v</sub> at 298 K,
- B. C<sub>v</sub> calculated at the current temperature T, that is, C<sub>vT</sub>,
- C. the rigorous value C<sub>v</sub><sup>\*</sup> calculated with equation (8), and
- D. the mean value of C<sub>v</sub> calculated with equation (10).

The first graphs, Figure 1a or 2a, show the heat capacity calculated at constant volume C<sub>v</sub>. The second graphs, Figure 1a or 2b, show the ratio of heat capacities computed using the same approximations. All calculations assume T<sub>0</sub> = 0K.

In addition to the standard quantities C<sub>v</sub> and γ, Figures 1 and 2 also show two other quantities, *error1* and *error2*. From equation (7), we calculate the error in the pressure when the value γ<sup>+</sup> is used instead of the exact γ\*. This relative error is given by the ratio

$$error1 = \frac{\gamma^+ - 1}{\gamma^* - 1} . \quad (12)$$

The quantity *error1* also represents the relative error in the calculated temperature because we are assuming ideal gases and the ideal gas law. The curves shown in Figures 1c and 2c are calculated with

- A. γ<sup>+</sup> = γ<sub>298</sub>, as in equation (9),
- B. γ<sup>+</sup> = γ<sub>T</sub>, that is, γ(T) at the current temperature, and
- C. γ<sup>+</sup> from equation (11).

Equation (11) might appear to be a good estimation of γ\*, but to compute γ<sup>+</sup> using this equation requires knowledge of the temperature in the term γ<sub>T</sub>. In order to determine how accurately γ<sub>T</sub> must be known in equation (11), we define the quantity *error2* in the following way. At the current temperature T<sub>c</sub>, we calculated *error1* from equation (12) by using γ<sup>+</sup> from equation (11), but now for three different temperatures, T, and T ± 200. We plot the maximum of these three values

$$error2(T_c, \gamma_{T_c}) = \max \left[ \left( \frac{\gamma^+(T) - 1}{\gamma^* - 1} \right)_{T=T_c-200}, \left( \frac{\gamma^+(T) - 1}{\gamma^* - 1} \right)_{T=T_c}, \left( \frac{\gamma^+(T) - 1}{\gamma^* - 1} \right)_{T=T_c+200} \right] .$$

Figures 1d and 2d thus show the largest error in pressure calculated with equation (7), when the temperature required to calculate the quantity γ<sub>T</sub> in equation (11) is known within a range of ± 200 K. The curves labelled '± 500' in the *error2* graphs have the same definition for range of temperatures ± 500.



### 3.3 Comments

The error in the pressure or temperature calculated with equation (7) and using a constant value of  $\gamma$  can be large. When calculations are carried out with  $\gamma_{298}$ , the error goes up to 25% for diatomic species and up to 50% for  $\text{H}_2\text{O}$ . The inaccuracy becomes especially significant for temperatures higher than 1000 K. The same error using the mean value  $\gamma^+$  from equation (11) is less than 5% in the whole range of temperature above 1000 K.

The use of an estimated temperature-dependent  $\gamma^+$  instead of a constant  $\gamma_{298}$  is more important when tri-atomic or multi-atomic molecules are involved (see  $\text{H}_2\text{O}$ ) because when the molecule has more degrees of freedom, the heat capacity has a stronger temperature dependence. For nonreactive flow, the assumption of constant  $\gamma_{298}$  is often satisfactory. Usually this kind of calculation involves air, that is a mixture of diatomic species, and the temperature does not increase as much as in a reactive flow.

When the phenomena studied are highly temperature dependent (for example, exothermic chemically reacting flow), an estimation of  $\gamma^*$  is necessary. Depending on the case studied, a rough estimation of  $\gamma_T$  and the use of equation (11) produces satisfactory estimates.

The evaluation of the quantity *error1* shows that the calculation of pressure using equation (7) is very sensitive to the temperature dependence of  $\gamma$ . Not including the temperature dependence can lead to an extremely inaccurate estimate of  $\gamma$ . However, for practical applications in the evaluation of pressure, the temperature dependence of  $\gamma_T$  does not have to be very accurate; a rough estimate is quite satisfactory, as shown from the values of *error2*.

## 4. A Detonation in a $\text{H}_2\text{-O}_2\text{-Ar}$ Mixture

In this section we will study the effect of including the temperature dependence of  $\gamma$  and the influence of the heat-release function on a computed detonation wave.

### 4.1 Numerical Model

The model solves the three basic conservation equations (mass, momentum, and energy) with a model for chemical reactions and heat release. The chemical model is a two-step model where the steps correspond to the chemical induction period and the heat-release period.

#### *Chemical Induction Period*

We keep track of the evolution of the chemical induction time by solving an equation of the form

$$\frac{\partial \tau_{ind}}{\partial t} = \frac{1}{t_{ind}(T(t), P(t))},$$

where  $\tau_{ind}$  represents the fraction of elapsed induction time and  $0 \leq \tau_{ind} \leq 1$ . The induction time  $t_{ind}$  is calculated for the local conditions of temperature and pressure and may be obtained by integrating a detailed set of reaction rates or from experimental data. In our case, we have used a set of data provided by Oran et al.<sup>1</sup> During the induction period, no energy is released.

#### Heat-Release Period

The exothermic chemical reaction is tracked by

$$\frac{\partial \tau_{hrel}}{\partial t} = \frac{1}{t_{hrel}},$$

where  $\tau_{hrel}$  represents the fraction of released energy and  $0 \leq \tau_{hrel} \leq 1$ . This progress parameter  $\tau_{hrel}$  is thus equal to  $\Delta U_R^o(t) / \Delta U_{R\ max}^o$ . The 'heat-release time' ( $t_{hrel}$ ) is either kept constant over the entire heat-release period or may evolve as a function of  $\tau_{hrel}$ . The function  $t_{hrel}(\tau_{hrel})$  may be obtained from kinetic calculations that integrate a set of elementary chemical reactions subject to the constraints of steady-state shock hydrodynamics.

#### 4.2 Cases Studied

The specific mixture studied is a  $H_2:O_2:Ar / 2:1:7$ , at an initial pressure and temperature of 50 Torr and 298 K, respectively. We have performed calculations for the eight different cases summarized in Table 1. Note that:

1. The heat-release time  $t_{hrel}$  is implemented in three different ways, that is,
  - a. fast reaction with constant rate:  $t_{hrel} = 5 \mu s$ ,
  - b. slow reaction with constant rate:  $t_{hrel} = 20 \mu s$ ,
  - c. variable rate  $t_{hrel}(\tau_{hrel})$  provided by a chemical kinetic computation in which the total heat-release time is 15–17  $\mu s$ .
2. The maximum amount of energy released is provided by the chemical kinetic computation, except in case 6. This case is discussed later.
3. The heat capacity ratio  $\gamma$  is either constant, in which case  $\gamma$  is equal to its initial value of 1.556, or  $\gamma$  evolves as a function of the progress parameter  $\tau$ , taking into account a temperature and species dependence of the heat capacity. This dependence is estimated by a preliminary kinetic computation.
4. The mean molecular mass,  $M$ , is either constant or a function of  $\tau$ , as is  $\gamma$ .
5. The induction time is tabulated as a function of temperature and pressure by integrating a full set of reaction rates. The purpose of cases 7 and 8 is to show the influence of the induction

**Table 1.** Physico-Chemical Parameters Used in Simulations

Case	$t_{hrel}$ [ $\mu$ s]	$\Delta U_{Rmax}^o$ [kJ/kg]	$\gamma$	$M$	$t_{ind}$
	(1)	(2)	(3)	(4)	(5)
1	const (5 $\mu$ s)	1010	const	const	–
2	const (20 $\mu$ s)	1010	const	const	–
3	$f(\tau_{hrel})$	1010	const	const	–
4	const (20 $\mu$ s)	1010	$f(\tau_{hrel})$	$f(\tau_{hrel})$	–
5	$f(\tau_{hrel})$	1010	$f(\tau_{hrel})$	$f(\tau_{hrel})$	–
6	const (10 $\mu$ s)	820	const	const	–
7	$f(\tau_{hrel})$	1010	$f(\tau_{hrel})$	$f(\tau_{hrel})$	$\times 1.5$
8	$f(\tau_{hrel})$	1010	$f(\tau_{hrel})$	$f(\tau_{hrel})$	$\times 2.0$
9	the fluid dynamics equations are solved with a full set of reaction rates and self-consistent heat capacities.				

time on the detonation propagation, so we have used the same conditions as in case 5 but multiplied the tabulated induction time by factors of 1.5 and 2.0, respectively.

6. Case 6 describes a calculation where all parameters ( $t_{hrel}$ ,  $\gamma$ , and  $M$ ) are kept constant and the total amount of energy released is artificially reduced.

For each case, we focus on the detonation velocity, the thickness of the induction zone and the thickness of the total reaction zone. The detonation velocity may be compared to the Chapman-Jouguet (CJ) value, that is, 1618 m/s.

In summary,

- Cases 1, 2, and 3 keep  $\gamma$  and  $M$  constant, and show the influence of heat release.
- Cases 4 and 5 show the influence of the temperature and species dependence of  $\gamma$  and  $M$ .
- Cases 7 and 8 show the influence of the induction time.
- Case 9 is a complete reference calculation with a full solution of the coupled fluid-chemical problem and a detailed set of elementary reaction rates.

### 4.3 Results and Comments

The initial conditions of the problem are a typical shock-diaphragm problem where the low pressure is 50 Torr (6666 Pa) and the driving gas is at an initial pressure and temperature of 2280 Torr (304,000 Pa) and 2300 K, respectively. After a few time steps, the mixture ignites and the shock velocity increases suddenly and strongly. After an initial relaxation, the velocity stabilizes and the result is a coupled shock front and reaction zone. Table 2 gives the values of the steady detonation velocity,  $D$ , the thickness of the induction zone,  $x_{ind}$ , and the reaction zone  $x_{react}$  for each case described above. Figure 3 shows results as a function of time for case 5. The maximum energy released in the calculation carried out with the full chemistry (case 9) is about 1080 kJ/kg, that is, a little more than the value used in the other calculations.

**Table 2.** Detonation Velocity and Structure of Simulations

case	1	2	3	4	5	6	7	8	9
$D$ (m/s)	1802	1787	1798	1649	1650	1626	1652	1655	1670
$x_{ind}$ (mm)	0.71	0.77	0.75	1.2	1.2	1.2	1.8	2.2	0.9/1.5
$x_{react}$ (mm)	4.1	13.3	12.2	12.9	11.8	7.4	11.8	12.5	-

Despite a significant difference in the heat-release time, the computations do not show any appreciable differences on the detonation velocity  $D$  among cases 1, 2, and 3 and between cases 4 and 5. However,  $D$  is quite high when the heat capacity ratio is kept constant. The induction zone is not affected by the heat release function and the total reaction-zone thickness evolves consistently with  $t_{hrel}$ .

The temperature and species dependence of  $\gamma$  and  $M$  modifies  $D$  dramatically (cases 4 and 5 compared to 1, 2, and 3). It is important to notice that allowing  $\gamma$  and  $M$  to be variable produces velocities close to the Chapman-Jouguet detonation velocity without any modification of the estimated amount of released energy. The results obtained with  $\gamma = f(\tau, T)$  agree well with the reference calculation, case 9.

Case 6 shows that it is possible to obtain the same qualitative result by keeping  $\gamma$  constant and decreasing the amount of released energy (in fact, by decreasing the fraction of reacted fuel). A reduction of the total heat released compensates for the thermal ideality of the mixture.

A relatively large variation of the induction time does not affect the steady detonation velocity.

However, the thickness of the induction zone is modified consistently by the change in induction time (cases 7 and 8).

The computations presented above and the results obtained are valid for this particular hydrogen-oxygen-argon mixture, and the observations and conclusions could be reasonably extended to similar mixtures. We are not sure, however, how the results generalize to other reactive systems. To help answer to this question, we now describe calculations for an "exotic" mixture for which experimental data are available.

### 5. Detonations in Mixtures Containing Fluorocarbons

The mixture considered is stoichiometric  $H_2-O_2$ , diluted 50% with Ar and  $CF_4$ , at an initial pressure and temperature of 200 Torr (26400 Pa) and 298 K, respectively. The computations have been carried out with 0, 5, 10, 15, and 20% of  $CF_4$ . Here there are many more kinds of chemical reactants and products than in the simple mixture of  $H_2$  and  $O_2$  discussed above. A possible kinetic mechanism and reaction rate constants are described by Nzeyimana and Van Tiggelen<sup>2</sup>. The advantage of testing our detonation computation using this mixture is that we have an extended set of experimental data provided by the Laboratoire de Physico-Chimie de la Combustion, Louvain-La-Neuve, Belgium. Moreover, an interesting feature of fluorocarbon compounds is that their heat capacity is much more temperature dependent than all of the species involved in the pure  $H_2-O_2$  mechanism.

**Table 3.** Experimental and CJ Detonation Velocities

Composition of Mixture: 33.33% $H_2$ , 16.66% $O_2$ , (50.00 - X)% Ar, X% $CF_4$					
X (% $CF_4$ )	0.0	5.0	10.0	15.0	20.0
$D_{CJ}$ (m/s)	1874	1875	1874	1872	1693
$D_{exp}$ (m/s)	1830	1859	1854	1829	1760

#### 5.1 Preliminary Observations

The behavior of explosive mixtures containing additional fluorocarbons is of interest because these compounds are thought to inhibit exothermicity in chemical reactions. However, there are some that behave more like promoters of detonation, such as  $CF_4$ , when less than 15% is added to the

reference mixture H<sub>2</sub>:O<sub>2</sub>:Ar / 2:1:3. Moreover, there is a notable difference between the experimental detonation velocity and computed CJ detonation velocity. Table 3 summarizes some of these results.

The major comment about the experimental results shown in Table 3 is that additional CF<sub>4</sub> slightly increases the detonation velocity, an effect that is not predicted by CJ calculations. Moreover, when a large amount (20%) of CF<sub>4</sub> is added, the experimental detonation velocity becomes surprisingly larger than the expected CJ value. To better understand the CF<sub>4</sub> behavior in detonation waves, calculations were done to test the chemical mechanism.<sup>3</sup> It is important to note that the kinetic mechanism of a reactive system involving CF<sub>4</sub> is not well known and most of the reaction rates involving CF<sub>4</sub> or one of its decomposition products are estimated. Nevertheless, these calculations showed that the products of the chemical reaction tracked by a kinetic mechanism are quite different than those predicted by a  $\gamma$  equilibrium calculations. One of the main assumptions of the CJ calculation is that the chemical reactions are in an equilibrium state, and it is this assumption that could explain why the CJ theory fails in this particular case. Taking this shift in composition into account, a larger amount of energy is released in the nonequilibrium kinetic calculation than in a calculation based on an equilibrium composition.

**Table 4.** Computed Detonation Velocity and Structure of Reaction Zone

Composition of Mixture: 33.33% H <sub>2</sub> , 16.66% O <sub>2</sub> , (50.00 - X)% Ar, X% CF <sub>4</sub>					
X (% CF <sub>4</sub> )	0.0	5.0	10.0	15.0	20.0
$D_{calc}$ (m/s)	1875.1	1923.2	1918.8	1871.5	1717.9
$x_{ind}$ (mm)	0.53	0.48	0.45	0.48	0.52
$x_{hrel}$ (mm)	1.09	1.08	1.06	1.19	1.13

## 5.2 Time-Dependent One-Dimensional Calculations

The detonation calculations are performed with the numerical model described above that takes account of the evolution of the ratio of the heat capacities,  $\gamma$ , and the mean molar mass,  $M$  as a function of the reaction progress parameter  $\tau_{hrel}$ . The heat release,  $\gamma$ , and  $M$  are related to  $\tau_{hrel}$  by a set of tabulated data provided by kinetic computation. In the mixture containing up to 15% CF<sub>4</sub>, the initial pressure and temperature in the driving gas section are 904,000 Pa and 3000 K, respectively. In the mixture containing 20% CF<sub>4</sub>, the calculation is performed with pressure and

temperature equal to 1,204,000 Pa and 3300 K, respectively. Table 4 summarizes the results, Figure 4 shows results of selected computations in more detail, and Figure 5 summarizes the detonation velocities predicted for different initial concentrations of  $\text{CF}_4$ .

### 5.3 Comments

The absolute differences between calculated detonation velocities and the experimental values may be due to a number of factors, such as the geometry of the shock tube or multidimensional effects. However, more significant is the way both the computed and experimental detonation velocities evolve with the addition of  $\text{CF}_4$ . With up to 15%  $\text{CF}_4$ , there is good agreement between the experimental data and the calculation. Moreover, the calculations help us to better understand the effect of adding  $\text{CF}_4$ .

The increase of the detonation velocity is the consequence of two competing effects:

1. Addition of  $\text{CF}_4$  causes an increase of the specific energy released compared with the reference mixture  $\text{H}_2:\text{O}_2:\text{Ar}$ .
2. The temperature behind the leading shock (von Neumann temperature) decreases when  $\text{CF}_4$  is added because the heat capacity of mixtures containing  $\text{CF}_4$  and its decomposition products ( $\text{CF}_3$ ,  $\text{CF}_2\text{O}$ , ...) is large.

The chemical model enables us to describe the interplay of these two effects as the amount of  $\text{CF}_4$  varies. This is particularly interesting because the model does not require the evolution of *all* participating chemical compounds to be followed. A elementary kinetic mechanism of reactive systems like  $\text{H}_2\text{-O}_2\text{-CF}_4$  involves at least 14 species and the integration of such a chemical mechanism is demanding in computer time. The trend observed when the mixture contains 20% is less satisfactory. One reason for this may be our poor knowledge of the chemistry of mixtures containing  $\text{CF}_4$  and the fact that the simulation is very sensitive to the total heat release and to the variation of  $\gamma$ , as shown in the first section of this work.

Mixtures with large amounts of  $\text{CF}_4$  are also more difficult to ignite, this is one of the effects of the large heat capacity of  $\text{CF}_4$ . The structure in the reaction zone fluctuates noticeably when there is over 10% of  $\text{CF}_4$ . Whether these oscillations are from a numerical origin or are a physical property of the system has not yet been investigated. However, they may be related to the increasing irregularity observed in multidimensional cellular structure of mixtures containing over 10%  $\text{CF}_4$ .

## 6. Conclusion

This work discusses the accuracy of selected input data used in computations of detonations. In particular we have considered the effect of including the temperature dependence of the heat capacity in the numerical model. The magnitude of the error made with constant  $\gamma$  is particularly large when the temperature is higher than 1000 K. This error increases substantially when chemical reactions modify the composition of the mixtures studied and produce multi-atomic compounds. A modified chemical model has been used in order to include a temperature-dependent  $\gamma$  in the computation. The model consists of a two-step chemical process but takes into account a relatively detailed description of the elementary chemical reaction rates. The model has been tested for the mixture  $\text{H}_2:\text{O}_2:\text{Ar}$  and compared successfully with other chemical models. Calculations of detonations in mixtures containing more complex species and involving a more complex chemical mechanism have been tested and show a good qualitative agreement with available experimental data. We therefore believe that this modified chemical model can be used for other reactive systems whose chemical kinetics is known to within a reasonable accuracy.

Some points remain unanswered. We do not know to what extent the kinetic calculations used to fit the set of data  $d\tau/dt$ ,  $\gamma$ , and  $M$  may influence the fluid dynamic model. We have used a kinetic mechanism related to the Raleigh line of the steady shock theory, but it would be interesting to investigate the effect of isothermal kinetics or kinetics at constant density. Two-dimensional calculations should be a good test of how accurately this model describes the chemistry occurring behind the shock wave.

## Acknowledgments

This work has been sponsored by the Naval Research Laboratory through the Office of Naval Research. The work was carried out during a NATO exchange program sponsored by the Department of Defence of Belgium.



## References

1. E.S. Oran, T.R. Young and J.P. Boris, Weak and Strong Ignition. I. Numerical Simulations of Shock Tube Experiments, *Combustion and Flame* 48, 135-148 , 1982.
2. E. Nzeyimana and P.J. Van Tiggelen, Influence of Tetrafluoromethane on Hydrogen Oxygen Argon Detonation, presented at 12th ICDERS, Ann Arbor, Mi, USA, 1989, published in *Prog in Astr. and Aero.*
3. M.H. Lefebvre, E. Nzeyimana, and P.J. Van Tiggelen, Influence of Fluorocarbons on H<sub>2</sub>-O<sub>2</sub>-Ar Detonations. Experiments and Modeling, presented at 13th ICDERS, Nagoya, Japan, 1991.

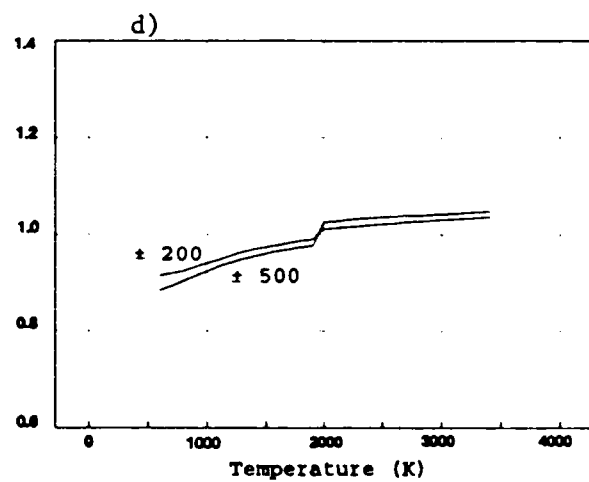
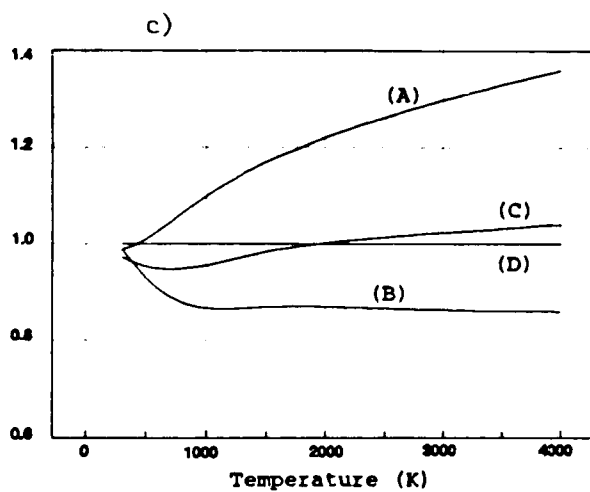
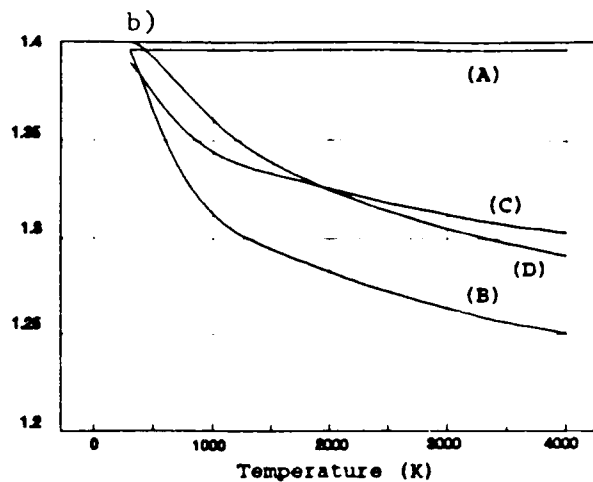
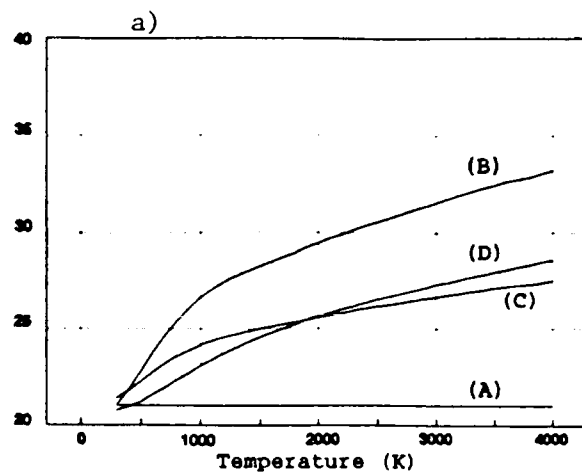


Figure 1. a) Heat capacity at constant volume ( $J/mol K$ ), b) ratio of specific heats,  $\gamma$ , c) *error1* (defined in text) and d) *error2* (defined in text) as a function of temperature for  $O_2$ .

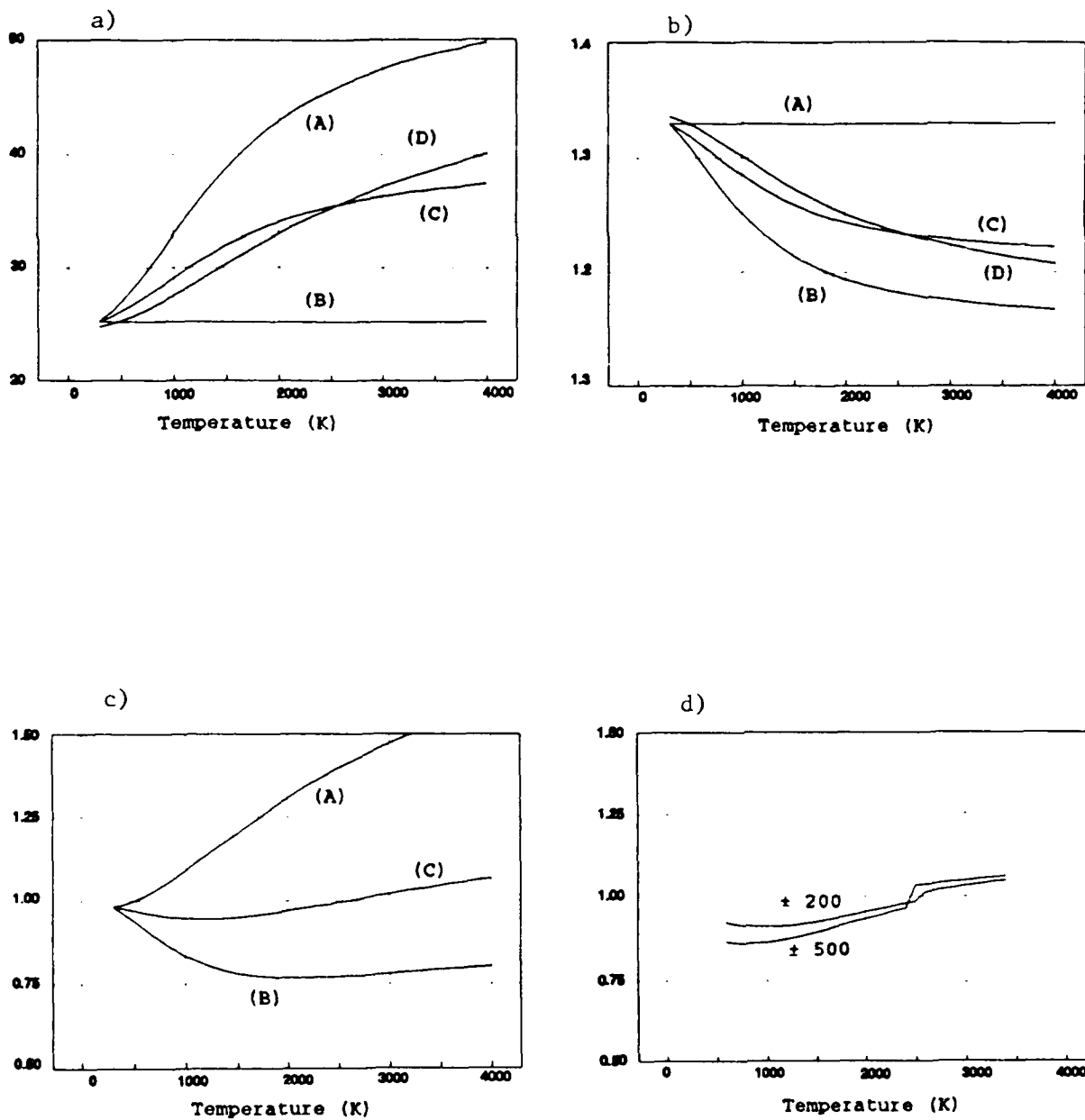
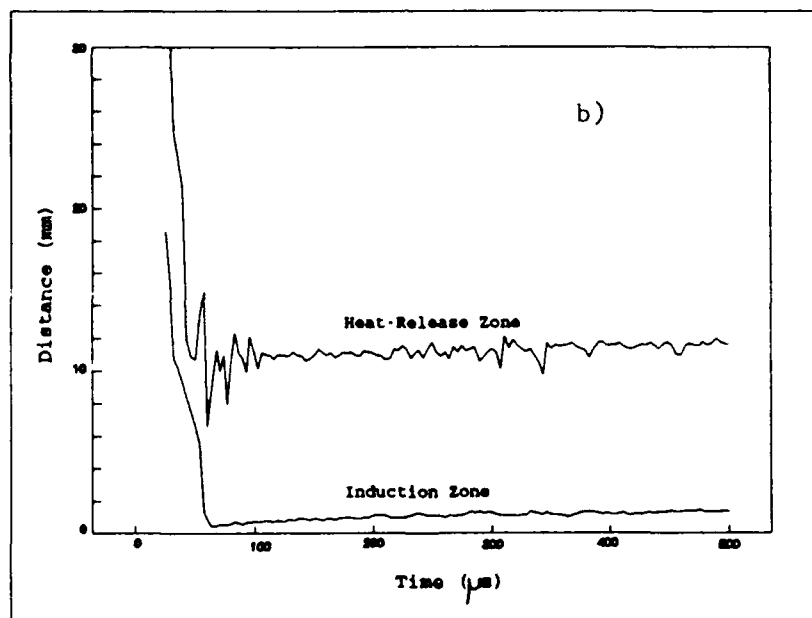
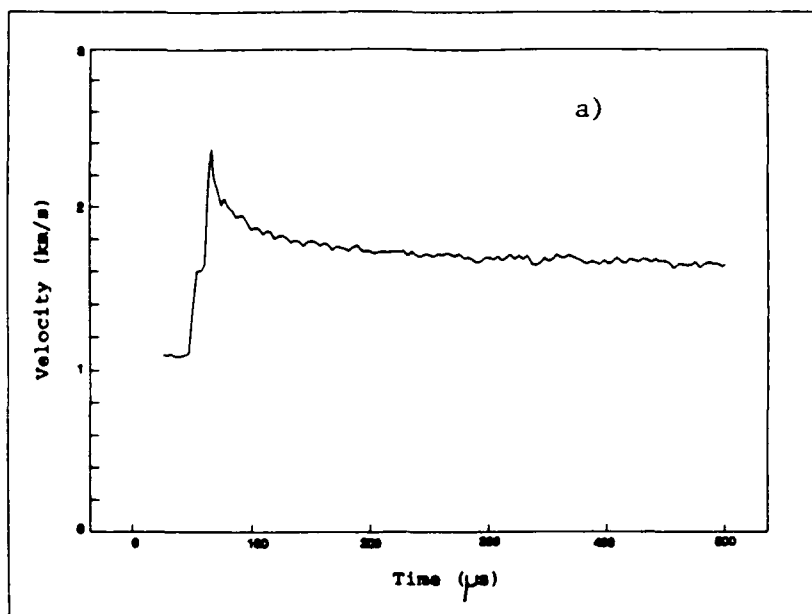
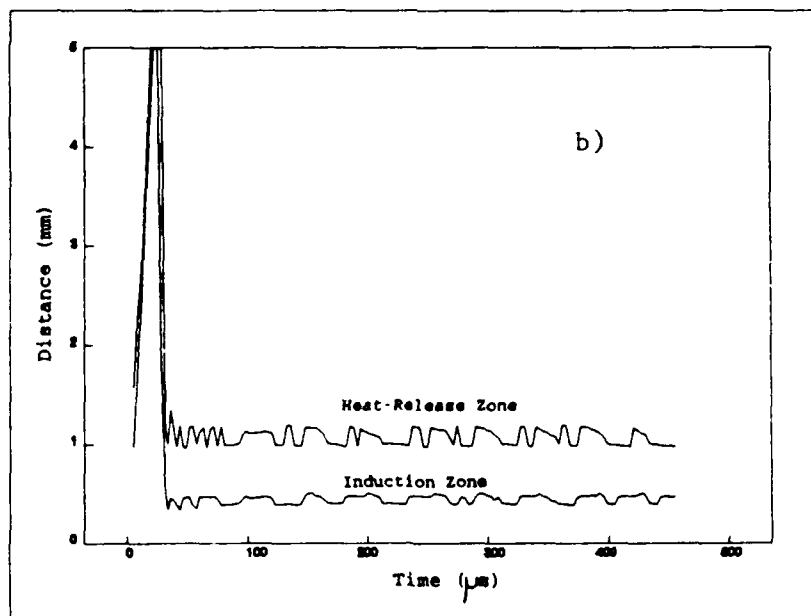
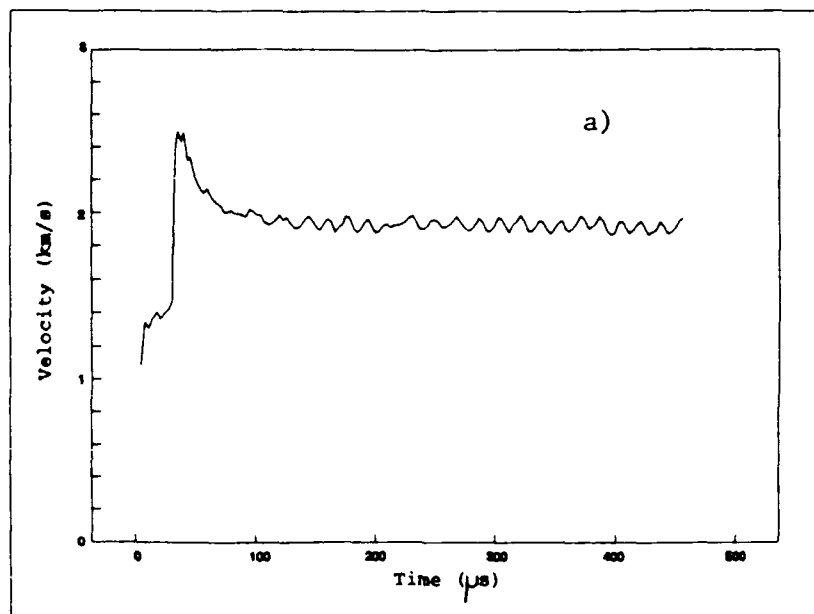


Figure 2. a) Heat capacity at constant volume (J/mol K), b) ratio of specific heats,  $\gamma$ , c) *error1* and d) *error2* as a function of temperature for H<sub>2</sub>O.



**Figure 3.** a) Detonation velocity and b) reaction zone as a function of time derived from a one-dimensional simulation of a detonation propagating in a mixture of  $H_2:O_2:Ar/2:1:7$  at 50 Torr and 298 K.



**Figure 4.** a) Detonation velocity and b) reaction zone as a function of time derived from a one-dimensional simulation of a detonation propagating in a  $\text{H}_2\text{-O}_2$  mixture containing 10%  $\text{CF}_4$  at 200 Torr and 298 K.

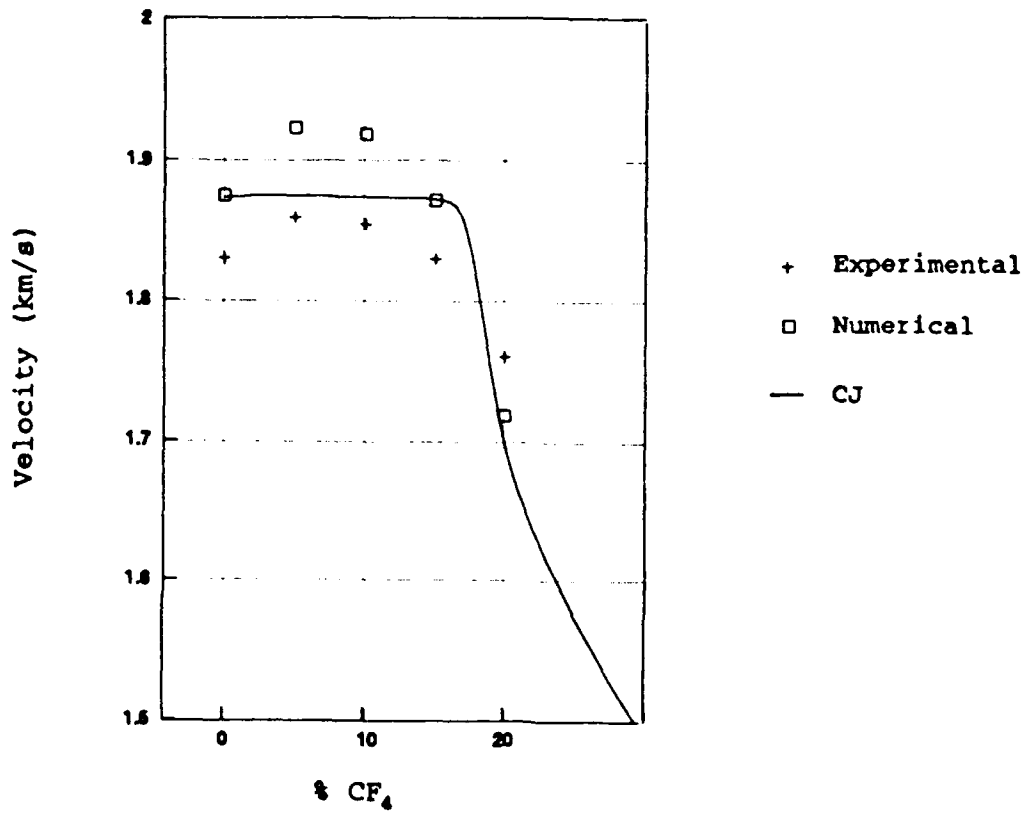


Figure 5. Numerical, experimental, and CJ detonation velocities in a H<sub>2</sub>-O<sub>2</sub> mixture as a function of the amount of added fluorocarbon.